SHAPE RECONSTRUCTION OF POLES AND PLATES FROM VEHICLE-BASED LASER SCANNING DATA

Hiroshi Masuda[1] , Shogo Oguri[2] and He Jun[2]
[1] Professor, Department of Mechanical Engineering and Intelligent Systems,
The University of Electro-Communications
1-5-1 Chofugaoka, Chofu, Tokyo 182-8585, Japan;
E-mail: masuda@sys.t.u-tokyo.ac.jp

[2] Master student, Department of Systems Innovation, The University of Tokyo
7-3-1 Hongo, Bunkyo-ku, Tokyo 113-8656, Japan;
E-mail: oguri@nakl.t.u-tokyo.ac.jp
E-mail: hejun@nakl.t.u-tokyo.ac.jp

KEY WORDS: shape reconstruction, point-cloud, geometry processing, mobile mapping

ABSTRACT: A vehicle-based laser scanner (VLS) can capture 3D point-clouds of road surfaces, buildings and roadside objects while running on the road. However, few researches have been done for reconstruct roadside objects, which consist of much small surfaces compared to roads and buildings. Roadside objects, such as utility poles, traffic signs, streetlights, guardrails, have to be maintained periodically. If 3D models of roadside objects can be efficiently constructed, they can be used for planning maintenance tasks without on-site survey. For reconstructing roadside objects, it is important to extract primitive surfaces such as planes and cylinders. However, it is difficult to stably extract surfaces from very noisy VLS data. In this paper, we propose a stable shape reconstruction method for relatively small poles and plates from noisy VLS data. Since the 2D projection of vertical poles and plates produce dense points, we extract points of them using the differences of point density. We extract dense regions using the Delaunay triangulation. Then we detect poles and plates from points in dense regions. Our method can detect surfaces even when objects attach with other objects, such as trees and shrubberies. By using detected surfaces, we reconstruct cylindrical poles, rectangular plates, circle plates and non-planar plates.

1. INTRODUCTION

A vehicle-based laser scanner (VLS) can capture 3D point-clouds of road surfaces, buildings and roadside objects while running on the road. While shape reconstruction of roads and buildings has been intensively studied so far, few research work have been done for roadside objects. It is not easy to extract surfaces of roadside objects, because roadside objects consist of much small surfaces compared to roads and buildings. Roadside objects include utility poles, traffic signs, streetlights, guardrails, and so on. Since there are a huge number of roadside objects in residential areas, their periodic maintenance tasks are very costly. If 3D models of roadside objects can be efficiently constructed from VLS data, they can be used for planning maintenance work without on-site survey.

For reconstructing roadside objects, it is important to extract primitive surfaces such as planes and cylinders. Surface extraction from a point-cloud has been intensively studied in computer-aided design and computer graphics. RANSAC and the least squares methods are commonly used for surface detection. However, it is not easy to detect small surfaces from very noisy, inaccurate and sparse VLS data. The quality of VLS data is very limited because of the inaccuracy of GPS, IMU, and calibration. In addition, the density of points is sparse in moving directions. In typical laser scanners mounted on vehicles, distances between scan lines are 6cm ~ 15cm when the rotation speeds of laser scanners are 75Hz ~ 200Hz. This density is not enough for small roadside objects.

Fortunately, most roadside objects consist of simple plates and poles, and they are placed vertically or horizontally. Although it is almost impossible to reconstruct general surfaces of small objects using a sparse point-cloud, it may be possible to extract a few known types of surfaces. In this paper, we focus on reconstructing shapes of poles and plates that are located vertically or horizontally.

Some researchers have studied to detect pole-like roadside objects. Lehtomaki, et al. (Lethomaki, 2010) detected pole-like objects by grouping scan-lines of each pole, because scan lines of a cylindrical pole are circular cross-sections. However, this method is unstable when a point-cloud is sparse and the radii of poles are small, such as streetlights.

Chen, et al. (Chen, 2007) clustered roadside objects by projecting points on a plane, and classified points using the principal component analysis. Yokoyama, et al. (Yokoyama, 2011) also detected poles and plates using the principal component analysis. They applied Laplacian smoothing for robustly detecting poles. The PCA method is powerful to estimate shapes of poles and planes, but it is based on correctly segmented points. However, it is not always possible to obtain correct segmentation. When multiple objects are grouped into the same segment, the PCA method often fails to adequately calculate characteristic eigenvalues for poles and planes. In Figure 1(a)(b), poles could not be correctly separated because an object is attached with other objects such as trees and shrubberies, and two objects are very closely located. These cases are not negligible in point-clouds of residential areas.

When we restrict shapes to vertical or horizontal surfaces, it is reasonable to project points on a 2D plane. Since the projections of cylinders and planes are circles and lines, respectively, the problem is to extract circles and lines from 2D points. Bolles, et al. (Bolles, 1981) detected cylinders by fitting a circle or an ellipse to projected points by using RANSAC. This method is useful for detecting poles from points of multiple objects. However, the RANSAC method may fail to detect correct shapes when point-clouds are very noisy. Figure 1(c)(d) show vertical projections of points. In these examples, pole-1 and pole-3 could not be detected using the RANSAC method; no circle was detected from Figure 1(c) and a wrong circle from Figure 1(d), as shown in Figure 1(e).

In this paper, we propose a stable shape reconstruction method for relatively small poles and plates from noisy VLS data. Our goal is to reconstruct object shapes rather than classifying object types, although our method is useful for classification. Since the projection of vertical poles and plates produce regions of high point density, we cluster points using the differences of point density. Then we detect primitive shapes from dense regions. In the following section, we explain point-clouds we used in this research, and then we show how to extract poles and plates in Section 3. Finally we conclude our research.

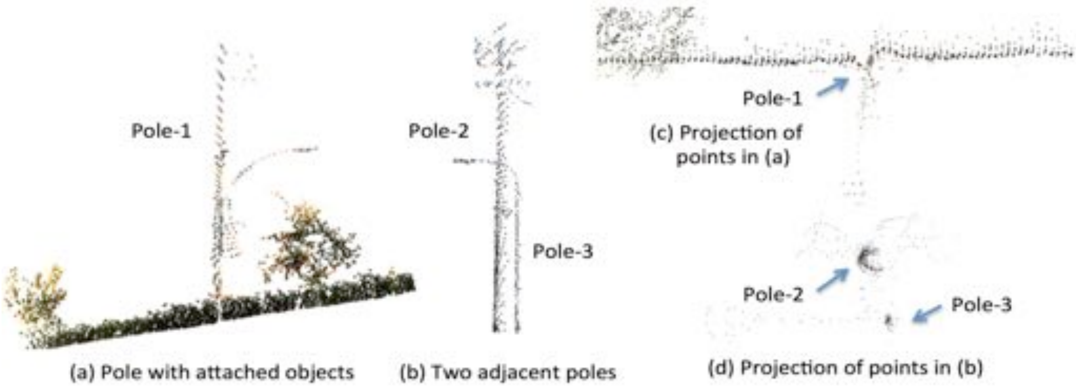

Figure 1: Points of roadside objects and their vertical projections.

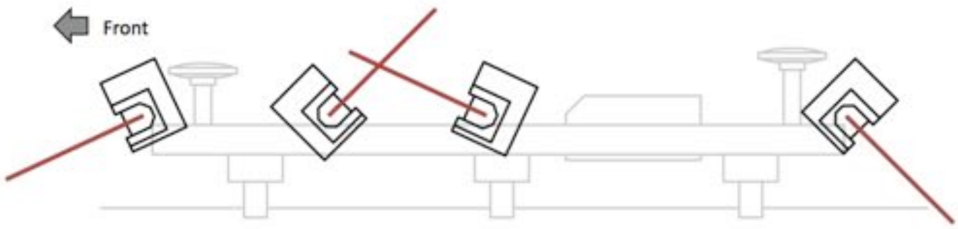

Figure 2: Mobile mapping system X-640

2. CLUSTERING OF POINT-CLOUDS

In this research, we used a MMS X-640 developed by Mitsubishi Electric Corporation. This MMS has 4 laser scanners (Sick LMS 291), which measure front upward, front downward, rear upward, and rear downward directions, as shown in Figure 2.

Laser scanners in upward and downward directions capture different scenes, as shown in Figure 3. While the upward data include utility poles, traffic signs, street lamps, and trees, the downward data contain road surfaces and partly include poles and other objects on road surfaces.

Figure 3 shows our process of clustering point-clouds. We exclude road surfaces from downward data, and the rest of points are merged with upward points. Road surfaces can be extracted using the z values and the slope of points in scan lines (He, 2012). Then we generate a kd-tree of the merged points. We search for k-nearest neighbors at each point and construct a k-nearest neighbor graph. Edges are defined when the distances of two points are less than threshold L_k. In this paper, we used L_k =35cm. Finally, a point-cloud is divided into groups of connected points. Many roadside objects are separated into different groups, but not a few objects are grouped with other objects when two objects are nearly located, as shown in Figure 1.

3. DETECTION OF POLES AND PLATES

3.1 Detection of High-Density Regions

Figure 4(a) shows points of a street lamp and a tree in the same group. Figure 4(b) shows their projection on a horizontal plane. When circles are searched for from projected points by using the RANSAC method, a wrong circle is detected as the optimum solution, as shown in this Figure. To solve this problem, we consider further subdividing points using the differences of point density.

When points are projected on a horizontal plane, vertical poles generate regions of high point density. In Figure 4(b), high-density regions represent the pole of the street lamp and the trunk of the tree. We apply Delaunay triangulation for separating high-density regions from other points. Figure 4(c) shows the triangulation of projected points. Two squares show high-density regions. In this triangulation, while sparse regions are connected by long

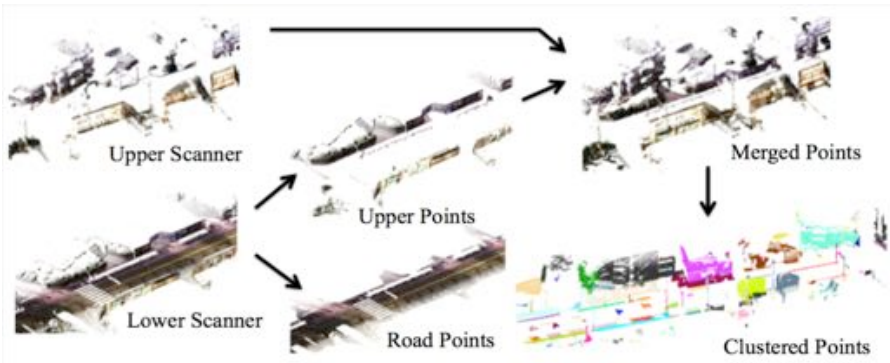

Figure 3: Clustering of point-clouds.

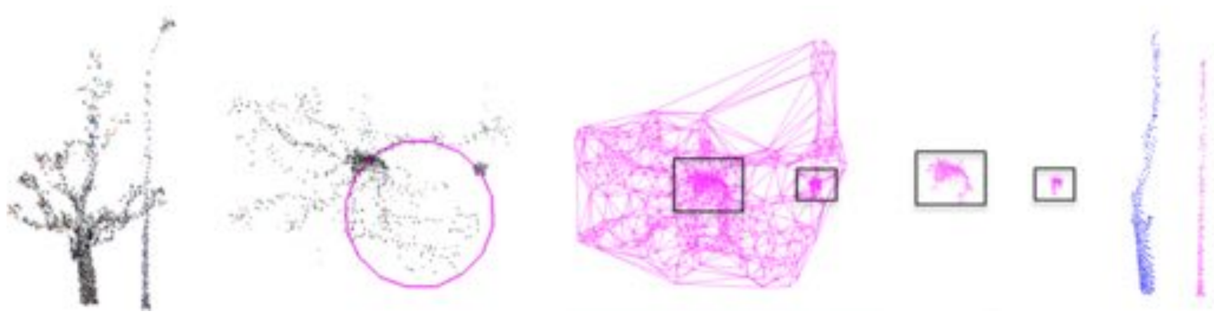

(a) 3D points (b) Projection (c) Triangulation (d) Dense regions (e) 3D points

Figure 4: Detection of Vertical Poles.

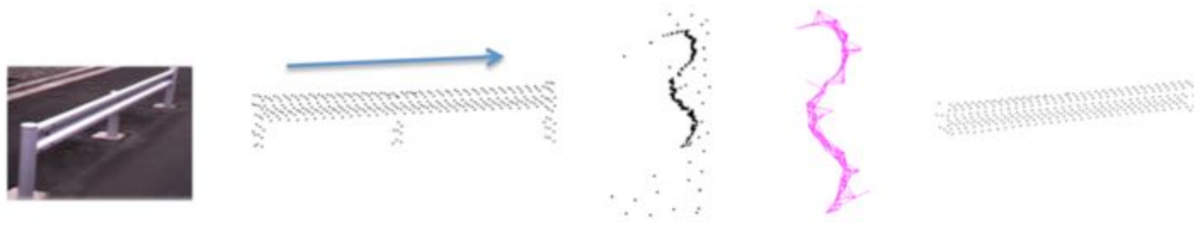

(a) Guardrail (b) 3D points (c) Projection (d) Dense region (e) 3D points

Figure 5: Detection of Horizontal Plates.

edges, high-density regions are connected by short edges. Therefore, we eliminate sparse regions by deleting triangles with long edges that the lengths are more than threshold L_t. Then we select connected components as high-density regions when more than N points are included in each connected component. Figure 4(d) shows two detected high-density regions. In this example, we used L_t=2mm, and N=30. Figure 4(e) shows original 3D points in high-density regions. 3D points of a trunk and a pole can be successfully extracted.

When the height of objects is small, we calculate the eigenvector with the maximum eigenvalue by applying the principal component analysis. Then we project points to the direction of the eigenvector. Figure 5 shows a guardrail on the road. Figure 5(d)(e) show an extracted high-density region and its 3D points, which represent the beam plate.

We can change threshold L_t adaptively when extracting high-density regions. Multilevel thresholds are useful, because the point density depends on the height or length of poles and plates. Figure 6 shows high-density regions detected using different thresholds. In our algorithm, we first extract high-density regions using a small threshold, and search for poles and plates in the high-density regions. Then we eliminate points in the detected high-density regions and extract high-density regions again using increased threshold. In our experiments, most poles could be extracted using L_t=2mm, and plates were extracted using L_t=4mm or 6mm for point-clouds of our MMS.

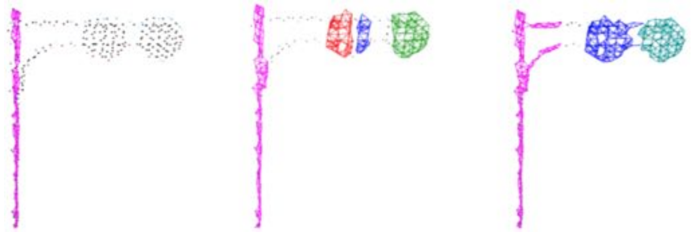

(a) L_t=2mm (b) L_t =4mm (c) L_t =6mm

Figure 6: Dense regions by different thresholds.

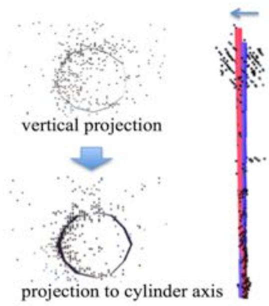

Figure 7: Correction of cylinder.

3.2 Detection of Poles

In our method, circles are searched for only from the dense regions using the typical RANSAC method. Three points are randomly selected and a circle equation is calculated. Then we count the number of neighbor points of the circle. This process is iterated many times and the circle equation with the maximum number of neighbor points is recorded. When the maximum number exceeds threshold M, the circle is regarded as a section of a cylinder. The height of the cylinder is determined using the range of neighbor points.

Since poles are usually not precisely vertical, we correct directions and radii. When a circle equation is determined, the direction of a cylinder can be calculated using neighbor points. We project points to the direction of the cylinder, and calculate high-density regions again. Figure 7 shows two projections and extracted cylinders. In this example, the projection by the cylinder axis increases the maximum number of neighbor points.

Figure 8 shows detected poles. In this example, a tall pole of a street lamp is extracted using a small threshold L_t=2mm, and a short trunk of a tree is extracted using L_t=4mm.

3.3 Detection of Planar Plates

Planar regions can also be extracted from high-density regions. Although planes can be extracted as lines in 2D projected points, we search for planes from 3D points of high-density regions, because the detection of lines is not

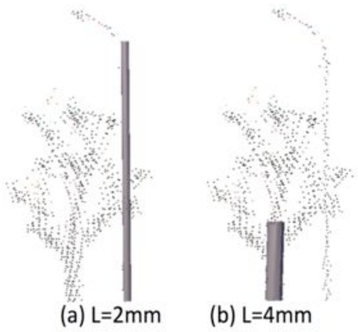

Figure 8: Detection of Cylinders.

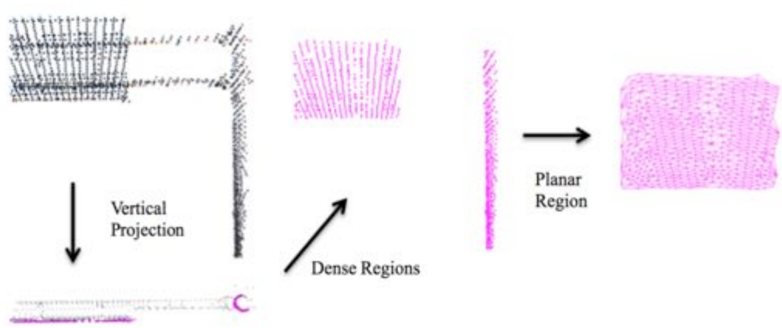

Figure 9: Extraction of Planar Plate

stable in our experiments. Figure 9 shows the process of plane detection. Points are projected on a horizontal plane, and high-density regions are selected. Then we generate a k-nearest neighbor graph using 3D points. In the k-nearest neighbor graph, edges are defined only when distances of two points are less than threshold L_k. We use a much larger value for L_k than the value L_t. We used L_k =35mm and L_t=2mm in this example. Then we apply the RANSAC method for detecting planar regions.

When planar regions are detected, we estimate the original shapes, as shown in Figure 10. For reconstructing a rectangle plate, we apply PCA to a planar region and align the direction of the plate to the main axis, as Figure 10(b). Then we determine the range of points along the eigenvectors.

The sizes of circle plates of traffic signs are determined by the Japanese standards. Here we prepare template circles with diameters of 40cm, 60cm, 90cm, and 120cm. For reconstructing a circle plate, we place a template circle at each point, and count the number of points inside the circle. We select the position at which the most points are included in the circle. Then we draw the fitted circle C, the inner circle C_i, the outer circle C_o, and the envelope rectangle R, as shown in Figure 10(c). Then we count the numbers of points inside the circles and the rectangle. We refer the number of points inside S as $num(S)$; the area of S as $area(S)$. The circle is tested whether the following conditions are satisfied:

$$num(C) > \alpha,\ \frac{area(C)\{num(C) - num(C_i)\}}{num(C)\{area(C) - area(C_i)\}} > \beta,\ \frac{area(C)\{num(C_o) - num(C)\}}{num(C)\{area(C_o) - area(C)\}} < \gamma,\ \frac{area(C)\{num(R) - num(C)\}}{num(C)\{area(R) - area(C)\}} < \delta,$$

where $\alpha, \beta, \gamma, \delta$ are thresholds. We used $\alpha = 50,\ \beta = 0.9,\ \gamma = 0.5,\ \delta = 0.7$ in this example. If the circle does not pass this test, it is discarded.

3.4 Detection of Non-Planar Plates

Figure 5 shows guardrails, which are very popular in Japanese residential areas. Since the beam plates of guardrails are not planar, we use the template of guardrails. As shown in Figure 11, we fit the template to points in high-density regions. When the point-set fits to the template, it is regarded as a beam plate of a guardrail. We used the sum of distances between the template and points for the metrics of fitting. When a beam is extracted, poles are extracted from the rest of points.

3.5 Experimental Results

Figure 12 shows some reconstructed shapes of roadside objects. Our method could successfully detect poles and plates. In the left case, support structures were also extracted as cylinders.

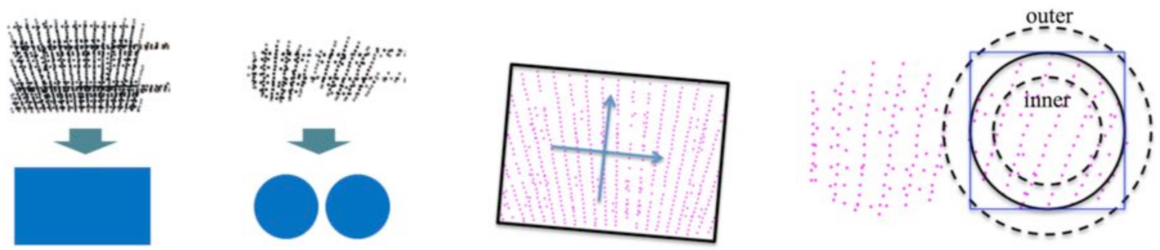

(a) Shape reconstruction (b) Rectangle plate (c) Circle plate

Figure 10: Reconstruction of plate shapes.

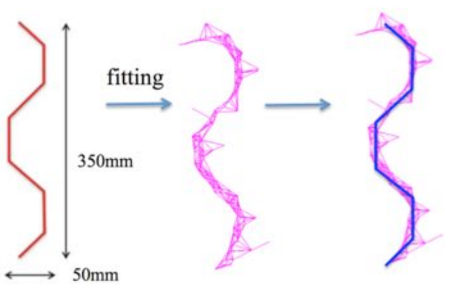

Figure 11: Reconstruction by a template.

Figure 12: Reconstruction of roadside objects.

We evaluated our method using practical VLS data. We first applied to 40 traffic signs with poles and plates. When the RANSAC method was applied without extracting high-density regions, poles and plates were extracted only from 11cases (27.5%), but our method could extract them from 31 cases (81.6%). We also extracted poles from large-scale point-clouds in residential areas (Figure 13). We extracted poles that are taller than 2m. We could extract 403 poles from 460 poles (87.6%). In this evaluation, the result showed that our method could extract poles from points in which multiple objects are included (Figure 14). However, our method failed to extract poles when points of poles are very sparse, or poles attaches with high-density regions.

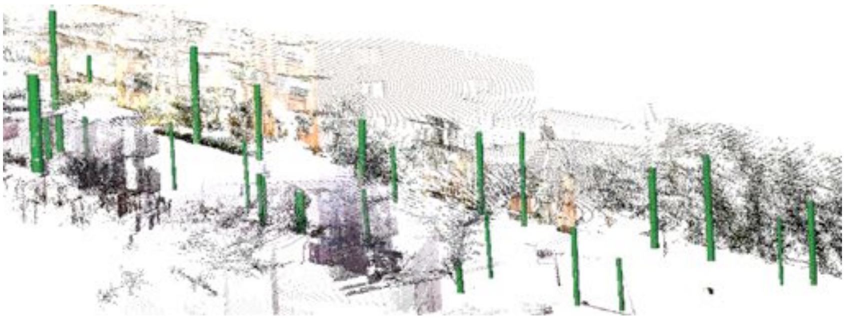

Figure 13: Detected Poles from a Point-Cloud.

Figure 14: Detected Poles in Points of Multiple Objects.

4. CONCLUSION

We proposed a method for robustly extracting poles and plates. We segmented points using differences of point densities and searched for surfaces in high-density regions. We also proposed a method for reconstructing rectangle plates, circle plates of traffic signs, and beam plates of guardrails.

In future work, we would like to improve the robustness of shape reconstruction. For improving our method, we plan to apply a graph-cut algorithm for detecting high-density regions more robustly. We also would like to evaluate the preciseness of radii of detected cylinders. In addition, since most roadside objects have known structure, we would like to reconstruct more complete shapes using flexible templates for streetlights, traffic signs, signals, and so on. Point-clouds in this paper were courtesy of Aisan Technology Cooperation. We would like to thank their support.

References

Bolles, R., Fischler, M., 1981. A Ransac-Based Approach to Model Fitting and Its Application to Finding Cylinders in Range Data. In: *International Conference on Artificial Intelligence, Vancouver, pp. 637-643.*

Chen, Y.-Z., Zhao, H.-J., Shibasaki, R, 2007. A Mobile System Combining Laser Scanners and Cameras for Urban Spatial Objects Extraction. In: *International Conference on Machine Learning and Cybernetics, Hong Kong.*

He, J., Masuda, H., 2012. Reconstruction of Roadways and Walkways Using Point-Clouds from Mobile Mapping System, In: *Asian Conference on Design and Digital Engineering*.

Lehtomäki , M., Jaakkola, A., Hyyppä, J., Kukko, A., Kaartinen, H., 2010. Detection of Vertical Pole-Like Objects in a Road Environment Using Vehicle-Based Laser Scanning Data, *Remote Sensing*, 2, pp. 641-664.

Mitsubishi Electric, 2012. http://www.mitsubishielectric.com/bu/mms/.

Yokoyama, H., Date, H., Kanai, S., Takeda, H., 2011. Pole-like Objects Recognition from Mobile Laser Scanning Data Using Smoothing and Principal Component Analysis, *ISPRS Workshop, Laser Scanning*, Volume XXXVIII, Calgary.